

Synthesis of Monodisperse Nanoparticles of Cobalt and Nickel Alloys in a Template Matrix of Layered Binary Hydroxide

KONSTANTIN A. TARASOV^{1,2}, VITALY P. ISUPOV¹, BORIS B. BOKHONOV¹ and ANATOLIY E. ERMAKOV³

¹*Institute of Solid State Chemistry and Mechanochemistry, Siberian Branch of the Russian Academy of Sciences, Ul. Kutateladze 18, Novosibirsk 630128 (Russia)*

E-mail: tarasov@solid.nsk.su

²*Novosibirsk State University, Ul. Pirogova 2, Novosibirsk 630090 (Russia)*

³*Institute of Metal Physics, Ural Branch of the Russian Academy of Sciences, Ul. S. Kovalevskoi 18, Ekaterinburg 620219 (Russia)*

Abstract

The nanosized particles of $\text{Ni}_{1-x}\text{Co}_x$ alloys encapsulated in a layered template matrix were synthesized by thermal decomposition of precursors – layered binary hydroxides $[\text{LiAl}_2(\text{OH})_6]_2\{(\text{Ni}_{1-x}\text{Co}_x(\text{edta})) \cdot q\text{H}_2\text{O}$. The morphology and the magnetic properties of the metal component were studied by X-ray phase analysis, electron microscopy (EM), and vibrational magnetometry. It was demonstrated by X-ray phase analysis that the resultant nanoparticles whose coherent scattering region (CSR) is 3–5 nm crystallize as a face-centred cubic (fcc) structure with a lattice parameter characteristic of $\text{Ni}_{1-x}\text{Co}_x$ alloys. EM studies revealed that in going from Ni to $\text{Ni}_{1-x}\text{Co}_x$ alloys (to $x = 0.86$) the particle morphology practically does not change; the particles are nearly spherical and do not range widely in size, their diameter increasing monotonously from 5.4 to 14 nm. In passing to Co ($x = 100$), however, the particles acquire discoid form and range widely in size, the average size being $d_{\text{av}} \sim 100$ nm. The results obtained demonstrated that variation of the composition of the precursor can be considered as a method of controlling the size and morphology of magnetic nanoparticles.

INTRODUCTION

During the last decade, interest in synthesis and investigation of the properties of nanosized particles of metals and their alloys has not declined. It is associated with the possibility to obtain promising functional materials and to solve the fundamental problems of research into new physical and chemical properties not inherent in bulk metals. The main difficulty encountered by experimenters is instability of metals in ultradisperse state. Therefore, interest is focused on the creation of compositions using oriented immobilization of nanosized particles in various stabilizing matrices. An approach using intercalated layered substances as precursors appears to hold much promise [1–9]. The capability of intercalation compounds to incorporate ions and molecules of various types makes it possible to modify the composi-

tion of the “host” matrix with new “guest” molecules and ions using “mild chemistry” methods. Moreover, due to the specific structure of intercalation compounds, having cavities and channels of preset geometry even in the initial state, the morphology of the resultant particles of the new phase is adjusted during chemical transformations; *i.e.*, this new phase plays the role of a so-called nanoreactor. It has been demonstrated that using layered binary hydroxides (LBH) with transition element complexes incorporated in their structure affords composites with metal nanoparticles of up to 5 nm in diameter and sizes ranging within very narrow limits during thermal decomposition [4, 7, 8]. It was established for the first time [8] that this approach can also be extended to nanoparticles of metal alloys. The importance of the result also lies in the fact that using an intercalation compound readily

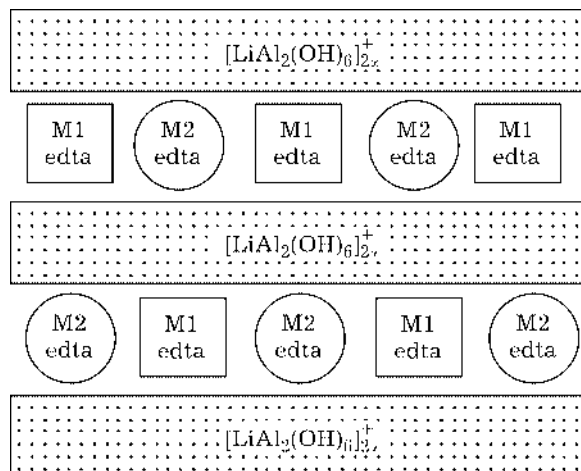


Fig. 1. X-ray diffraction pattern of $[\text{LiAl}_2(\text{OH})_6]_2\{\text{Ni}_{0.55}\text{Co}_{0.44}(\text{edta})\} \cdot q\text{H}_2\text{O}$.

afforded a precursor with two transition elements and homogeneous phase composition. Thus even in the starting compound, the M1^{2+} and M2^{2+} cations were “mixed” at the molecular level, which favors the formation of $\text{M1}_{1-x}\text{M2}_x$ binary mixtures through reduction of Ni^{2+} , Co^{2+} , and Cu^{2+} cations (Fig. 1). The stabilizing template matrix, in which nanoparticles of metals and their alloys were encapsulated, was mixed lithium and aluminum oxides and the carbon-containing product, which remained after thermal decomposition of $[\text{LiAl}_2(\text{OH})_6]^+$ hydroxide layers and the edta organic ligand, respectively.

The purpose of this work is further study of the morphological and magnetic properties of nanoparticles of nickel and cobalt alloys using precursor compounds based on layered binary hydroxides.

EXPERIMENTAL

The precursor compounds based on layered binary aluminum and lithium hydroxide used in this work, $[\text{LiAl}_2(\text{OH})_6]_2\{(\text{M}^1\text{M}^2(\text{edta}))\} \cdot q\text{H}_2\text{O}$, where M^1 and M^2 are the Co^{2+} and/or Ni^{2+} cations; edta is the four-charged anion of ethylenediaminetetraacetic acid (below LBH- $\text{Ni}_{1-x}\text{Co}_x$), were synthesized by treatment of $[\text{LiAl}_2(\text{OH})_6]\text{Cl} \cdot 1.5\text{H}_2\text{O}$ with water solutions of $\text{Na}_2[\text{Ni}(\text{edta})]$ and $\text{Na}_2[\text{Co}(\text{edta})]$ salts taken in an appropriate ratio according to the procedure described in [10]. The solid $\text{Na}_2[\text{M}(\text{edta})] \cdot z\text{H}_2\text{O}$ ($\text{M} = \text{Ni}, \text{Co}; z = 2-4$) were obtained by the procedure described in [11]. The chemical composition (Li, Na, Al, Co, Ni, Cu, Cl) of the compounds was analyzed using the standard procedure. The total contents of the transition elements in LBH- $\text{Ni}_{1-x}\text{Co}_x$ are given in Table 1. The content of the adsorbed and interlayer water ($q\text{H}_2\text{O}$ in the general formula) depends on the atmospheric humidity and changes in the range $q = 3-4$.

Thermal decomposition was carried out in an evacuated test tube of heat-resistant glass placed in an electric furnace. Heating was applied at a constant rate of $5^\circ\text{C}/\text{min}$ to 450°C ; then the sample was kept at this temperature for 2 h. Heating and subsequent cooling were conducted in a mode of permanent pumping-out with a vacuum forepump in vacuum of 1–4 Pa. After calcination, mass loss measured with an analytical balance varied in the range 45–50 % for the whole series of samples.

The phase composition was analyzed on DRON-3 and DRON-4 X-ray diffractometers

TABLE 1

Content of divalent metals in LBH- $\text{Ni}_{1-x}\text{Co}_x$ precursor compounds

Ni : Co ratio in solution	Content, mass %		Ni : Co atomic ratio
	Ni	Co	
9 : 1	9.60	0.87	11.1
3 : 1	5.59	1.25	4.49
2 : 1	4.95	1.91	2.60
1 : 1	4.23	3.34	1.27
1 : 2	2.92	4.10	0.71
1 : 3	2.53	4.90	0.52
1 : 9	1.40	8.80	0.16

using CoK_α and CuK_α radiation, respectively. To estimate the size of the coherent scattering region (CSR), X-ray diffractograms were recorded at a rate of $0.5^\circ(2\theta)/\text{min}$; crystalline germanium was used as a standard. Electron microscopic (EM) images were obtained with a Jeol JEM-2000 FXII high-resolution electron microscope. Magnetization curves were recorded at ambient temperature using a vibrating magnetometer in quasistatic fields with intensities of up to $22 \cdot 10^5 \text{ A/m}$ (27 kOe).

RESULTS AND DISCUSSION

Synthesis of $\text{LBH-Ni}_{1-x}\text{Co}_x$

After treatment of the chloride derivative of lithium-aluminum layered binary hydroxide $[\text{LiAl}_2(\text{OH})_6]\text{Cl} \cdot 1.5\text{H}_2\text{O}$ with aqueous solutions containing both $\text{Na}_2[\text{Ni}(\text{edta})]$ and $\text{Na}_2[\text{Co}(\text{edta})]$ in different ratios, chemical analysis of the products showed that two divalent metals had appeared in the solid phase. Their atomic ratios were close to the atomic ratios set for the initial solution (see Table 1); however, the Co : Ni ratio in the solid product was slightly smaller than in solution. This indicates that nickel is a slightly better substituent for chloride ions than cobalt.

The diffractograms of $[\text{LiAl}_2(\text{OH})_6]_2\{(\text{Ni}_{1-x}\text{Co}_x(\text{edta}))\} \cdot q\text{H}_2\text{O}$ are practically identical to each other and repeat the diffractograms of $[\text{LiAl}_2(\text{OH})_6]_2\{(\text{M}(\text{edta}))\} \cdot p\text{H}_2\text{O}$ containing complexes of one transition element [8]. This is not surprising since the $[\text{Ni}(\text{edta})]^{2-}$ and $[\text{Co}(\text{edta})]^{2-}$ chelators are identically charged and have close geometry characteristics. The diffractogram of one of the compounds from the series of $\text{LBH-Ni}_{1-x}\text{Co}_x$ is given in Fig. 1. It can be inferred that these anions are statistically mixed when incorporated in the interlayer space of the LBH structure from solution, as is schematically illustrated by Fig. 2; this should promote easy formation of a solid solution of cobalt and nickel during their simultaneous reduction.

Microstructure

After thermal decomposition of $\text{LBH-Ni}_{1-x}\text{Co}_x$, the phase composition of these compounds changes similarly to the case of LBH-Ni and LBH-Co [4, 7, 8]: after dehydration of the hydroxide matrix above 300°C , amorphization of the product occurs. In the subsequent process, after decomposition of the organic fragment and reduction of the transition element cations above $400\text{--}450^\circ\text{C}$ (XRPA data),

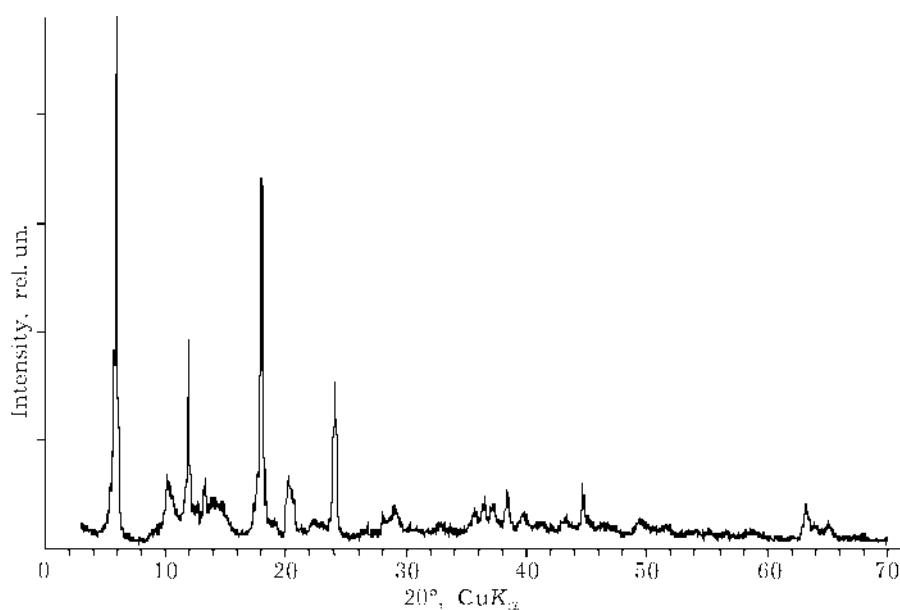


Fig. 2. Schematic diagram of the structure of lithium-aluminum layered binary hydroxide containing $[\text{M}^1(\text{edta})]^{2-}$ and $[\text{M}^2(\text{edta})]^{2-}$ anions.

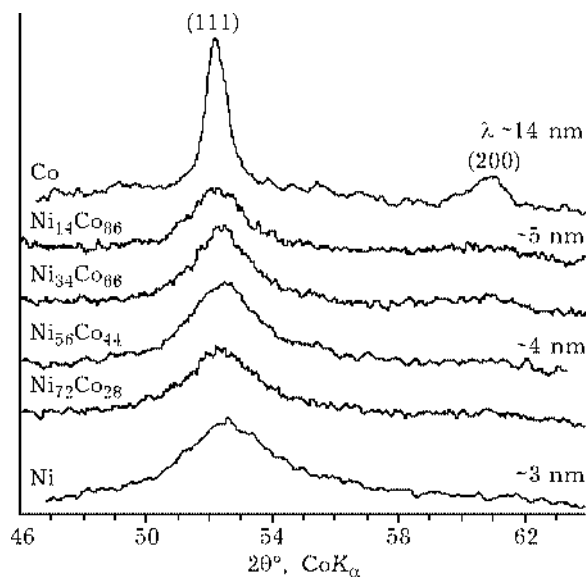


Fig. 3. Diffractograms of the products of thermal decomposition for LBH-Ni_{1-x}Co_x in vacuum at 450 °C.

a metal phase appeared in the cubic modification for both metals.

As can be seen from X-ray profiles (Fig. 3), the reflection indexed as (111) in a face-centred cubic structure shows strong broadening for the whole series of products. This may be due to the presence of the metal phase in the nanocrystal state. The second most intense reflection, (200), is observed only for “pure” cobalt. In the whole series of SS-LBH-Ni_{1-x}Co_x samples, the *a* parameter of the metal, which was found from the *d*₁₁₁ interplane distance, is in good correlation with Vegard’s law (Fig. 4). The deviation of the experimental points from the curve that connects the points corresponding to the reference values is attributable to a significant mistake in determining *a* and probably to changes in the structural parameters of metals and alloys from bulk to nanocrystal state.

As is known, cobalt and nickel can easily form with each other a continuous series of solid solutions; therefore, one can argue that SS-LBH-Ni_{1-x}Co_x samples contain alloys with these metals. The value of CSR estimated from the broadening of the (111) reflection suggests that in going from “pure” nickel to its alloy (to Ni_{0.14}Co_{0.86}) the size of the crystallite changes slightly, increasing from ~3 to ~5 nm (Fig. 3). However, in passing to cobalt the size of the CSR increases sharply to ~14 nm.

This sudden result is confirmed by an electron microscopic study. The EM micrograph of the SS-LBH-Ni_{0.56}Co_{0.44} sample shows that the alloy particles are spherical and have a very small size with a very narrow distribution, repeating the morphology of nickel particles in the SS-LBH-Ni sample [7, 8]. The average diameter of Ni_{0.56}Co_{0.44} alloy particles increases insignificantly, approximately from 5 to 8 nm (Fig. 5). As the cobalt content of particles increases in alloys up to Ni_{0.34}Co_{0.66} and Ni_{0.14}Co_{0.86}, the particle diameter grows monotonously, reaching ~11 and 14 nm, respectively, with a very narrow scatter of size. Analysis of pictures in different projections demonstrates that the Ni_{0.14}Co_{0.86} particles clamped between the layer packages are of slightly oblate spherical form. The picture changes drastically in going to the sample with “pure” cobalt: the average diameter of particles increases sharply to ~100 nm with a wide scatter of size (10–200 nm). The particle shape also changes; the particles located deep in the matrix show clearly defined discoid form. The reason for this change in the morphology of particles from Co to Ni_{1-x}Co_x is yet to be explained. This cannot be attributed merely to dilution as, for example, can be done for the SS-LBH-Cu_{0.45}Co_{0.55} system, where alloy formation was not observed and metal particles were not substantially different from those of “pure” SS-LBH-Cu and SS-LBH-Ni systems [8]. The similarity in

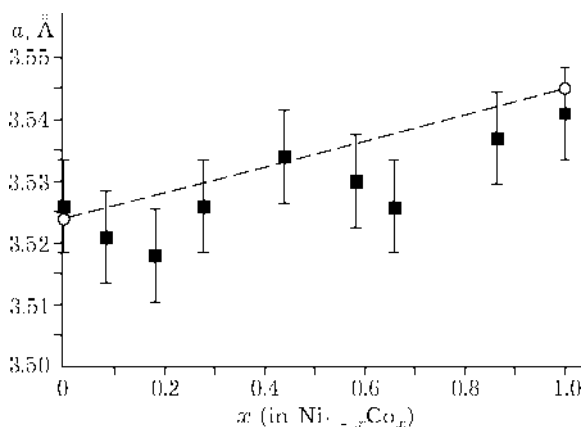


Fig. 4. Dependence of the unit cell parameter on the composition (Vegard’s law) for nanoparticles of Ni_{1-x}Co_x alloys in the products of thermal decomposition. The dashed curve connects the points corresponding to the reference values of the unit cell parameters for bulk Ni⁰ (cubic close-packed cell) and Co⁰ (hexagonal close-packed cell).

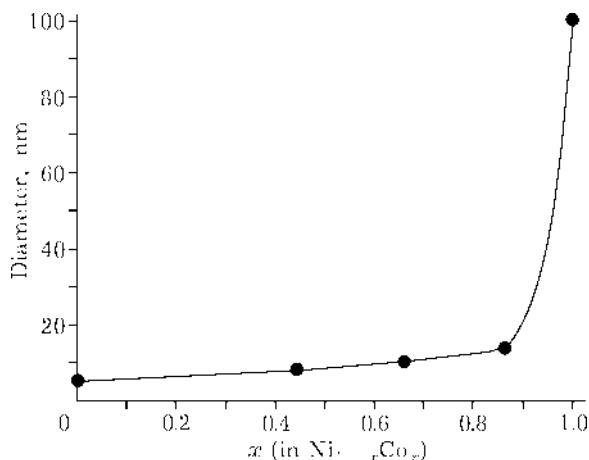


Fig. 5. Dependence of the average diameter of the nanoparticles of $\text{Ni}_{1-x}\text{Co}_x$ alloys on composition.

morphology between the $\text{Ni}_{1-x}\text{Co}_x$ and Ni particles can be attributed to the peculiarity of nickel nucleating centres, acting as centres of growth for alloy particles.

Magnetic measurements

According to magnetic weighing data, magnetization of the product increases in nickel-cobalt samples with increased contents of cobalt, which typically has higher values of magnetic moment than nickel (Fig. 6). For both "pure" Co and Ni and their alloys, magnetiza-

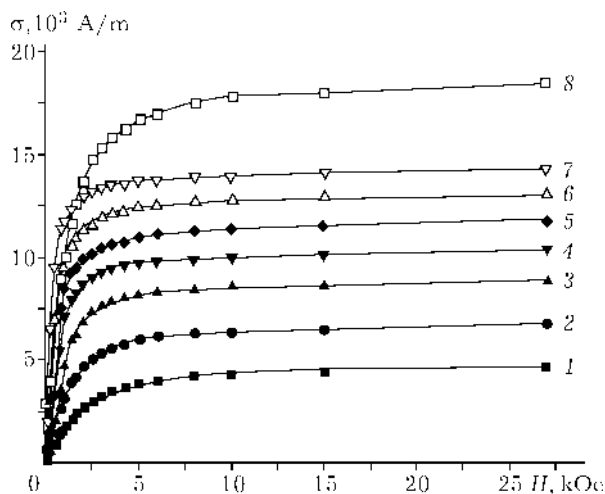


Fig. 6. Dependence of magnetization σ on the intensity of the magnetic field H for the thermally treated samples (registration temperature 20°C): 1 - LBH-Ni, 2 - LBH- $\text{Ni}_{0.92}\text{Co}_{0.08}$, 3 - LBH- $\text{Ni}_{0.82}\text{Co}_{0.18}$, 4 - LBH- $\text{Ni}_{0.72}\text{Co}_{0.28}$, 5 - LBH- $\text{Ni}_{0.56}\text{Co}_{0.44}$, 6 - LBH- $\text{Ni}_{0.42}\text{Co}_{0.58}$, 7 - LBH- $\text{Ni}_{0.14}\text{Co}_{0.86}$, 8 - LBH-Co.

tion normalized to the content of magnetic metal in SS-LBH- $\text{Ni}_{1-x}\text{Co}_x$ was 60–86 % of the tabulated values of σ_{sat} for bulk metals and their alloys even in a field with magnetization $H = 27$ kOe. This deviation is not surprising, since saturation magnetization of nanocrystal ferromagnets (when saturation is attainable) often appears to be less significant compared to bulk materials, sometimes differing several fold [12]. The extent of this difference may depend on the particle shape and size, amount of impurities in the metal, temperature of measurements, etc. The form of the magnetization curves, showing a long region of transition to the saturation plateau, may also point to the fact that these particles are nearly superparamagnetic. This is quite typical for magnetic metals whose particles are close to the critical size $r \sim 10$ nm, which is the typical dimension of the magnetic domain.

CONCLUSIONS

This investigation, aimed at synthesis of nanoparticles of nickel and cobalt alloys, has demonstrated that using layered intercalation compounds as precursors makes it possible to readily obtain particles of required composition. The result was unexpected and promising because it showed that variation of the alloy composition gives rise to dramatic changes in the morphology of nanoparticles. This can be considered as one of the ways of controlling particle size of ferromagnetic metals, directly governing the magnetic characteristics such as the strength of the coercive field, magnetization of saturation, blocking temperature, etc. The results obtained can be extremely useful to chemists and physicists who work on the problem of obtaining magnetic materials with specified properties.

Acknowledgement

This work was supported by the Russian Fund for Basic Research grant No. 02-03-32066, Ministry of Education of the Russian Federation and CRDF grant No. Y1-B-0813, and "National Science Support Foundation".

REFERENCES

- 1 T. Sato, H. Okuyama, T. Endo and M. Shimada, *Reactivity of Solids*, 8 (1990) 63.
- 2 V. P. Isupov, K. A. Tarasov, L. E. Chupakhina *et al.*, *Dokl. Ross. Akad. Nauk*, 336, 2 (1994) 209.
- 3 V. P. Isupov, K. A. Tarasov, L. E. Chupakhina *et al.*, *Zhurn. Neorg. Khim.*, 40, 1 (1995) 22.
- 4 V. P. Isupov, L. E. Chupakhina, R. P. Mitrofanova *et al.*, *Solid State Ionics*, 101–103 (1997) 265.
- 5 J. Walter and H. Shioyama, *Phys. Letters A*, 254 (1999) 65.
- 6 A. V. Lukashin, S. V. Kalinin, A. A. Vertegel *et al.*, *Dokl. Ross. Akad. Nauk*, 369, 6 (1999) 781.
- 7 K. A. Tarasov, V. P. Isupov, A. E. Yermakov *et al.*, *Solid State Phenomena*, 90–91 (2003) 527.
- 8 K. A. Tarasov, V. P. Isupov, B. B. Bokhonov *et al.*, *J. Mater. Synth. Proc.*, 9 (2000) 21.
- 9 O. Santini, D. H. Mosca, W. H. Schreiner *et al.*, *J. Phys. D: Appl. Phys.*, 36 (2003) 428.
- 10 K. A. Tarasov, D. O'Hare, and V. P. Isupov, *Inorg. Chem.*, 42 (2003) 1919.
- 11 V. A. Radko and E. M. Ekimets, *Zhurn. Neorg. Khim.*, 7 (1962) 683.
- 12 Yu. I. Petrov, *Klustry i malye chastitsy*, Nauka, Moscow, 1986.